

SP2016\_3124805

# MODELLING OF THE CYCLIC AND VISCOPLASTIC BEHAVIOR OF A COPPER-BASE ALLOY USING CHABOCHE MODEL

Wissam BOUJILA<sup>(1)</sup>, Jörg RICCIUS<sup>(1)</sup>

<sup>(1)</sup> German Aerospace Centre – DLR Lampoldshausen, Langer Grund, D-74239 Hardthausen (Germany), Email: [wissam.bouajila@dlr.de](mailto:wissam.bouajila@dlr.de), [joerg.riccius@dlr.de](mailto:joerg.riccius@dlr.de)

**KEYWORDS:** Chaboche model, cyclic behavior, viscoplastic behavior, static recovery, parameters determination.

## ABSTRACT:

A step-by-step procedure for the identification of the Chaboche model's parameters applied to a copper-base alloy that may be considered as a cost efficient material for a rocket engine combustion chamber inner liner is presented in this paper. Experimental data from a strain-controlled uniaxial low cycle fatigue test and a stress relaxation test are used for the identification of the model's parameters. In addition to the fatigue test and the stress relaxation test, a dwell test with a hold period of 600 s at extreme strain amplitude in tension and in compression is considered for the assessment of the accuracy of the identified model parameters. The comparisons of the predictions of the model with optimized parameters to the above mentioned experiments at 900 K for the considered copper-based alloy are presented.

## 1 INTRODUCTION

The strong demand for light-weight structures for space transportation systems leads to a close-to-the-limit design of the components – including the rocket engine. The inner liner of a regeneratively cooled wall of a main stage rocket combustion chamber is extremely loaded by the high temperature of the hot gas and the pressure difference between the coolant and the hot gas. An understanding of the material behaviour at such conditions is very important for the fatigue life prediction of the structure.

Among the several viscoplasticity constitutive models proposed for predicting material behaviors at high temperatures, the unified Chaboche viscoplasticity model has been widely accepted. The unified Chaboche constitutive model has received much

attention due to its simplicity to comprehend and use. The Chaboche model is capable of simulating cyclic plasticity, strong deformation rate effects, and other time dependent processes such as creep, stress relaxation and static/dynamic recovery.

Although the Chaboche model is widely used, few references in literature [1] [2] provide detailed information on whose tests have to be carried out and how one has to process the experimental data to determine a complete set of material parameters to be used within the model.

The purpose of the present paper is to provide the reader with an as detailed as possible guideline on the identification of the unified Chaboche model using uniaxial tests data. A step by step procedure in the characterization of the model parameters is suggested.

A copper base alloy that may be used as a cost efficient material for a rocket engine combustion chamber inner liner is considered for this work. Experimental data from a strain-controlled uniaxial low cycle fatigue and from a uniaxial stress relaxation test are used to illustrate the material parameter identification procedure.

In addition to the fatigue test and the stress relaxation test, a strain-controlled uniaxial dwell test with holding periods in tension and compression is considered for the assessment of the accuracy of the identified model parameters. The comparison of the predictions of the model with the optimized parameters to the data from the above mentioned tests at 900 K are presented in this paper.

## 2 MATERIAL MODEL

### 2.1 Constitutive equations of the unified Chaboche model

The decomposition of the total strain rate can be assumed as

$$\dot{\epsilon} = \dot{\epsilon}_e + \dot{\epsilon}_{th} + \dot{\epsilon}_{vp} \quad (1)$$

with  $\dot{\epsilon}_e$  the elastic strain rate,  $\dot{\epsilon}_{th}$  the thermal strain rate, and  $\dot{\epsilon}_{vp}$  the rate of the inelastic strain except the thermal strain.

At a constant temperature ( $\dot{\epsilon}_{th} = 0$ ) and within the uniaxial small-strain hypothesis, the resulting stress increment  $\dot{\sigma}$  is given in equation (2) according to Hook's law for an isotropic elastic material:

$$\dot{\sigma} = E(\dot{\epsilon} - \dot{\epsilon}_{vp}) \quad (2)$$

with  $E$  the Young's modulus of the material.

The uniaxial form of the Chaboche model as described in [3] is adopted in the present paper. The evolution of the inelastic strain is defined as a function of the external stress  $\sigma$  and internal variables such as the back stress  $\chi$ :

$$\dot{\epsilon}_{vp} = \dot{p} \operatorname{sgn}(\sigma - \chi) \quad (3)$$

with the cumulated inelastic strain increment  $\dot{p}$  given by a Norton type law

$$\dot{p} = \left\langle \frac{f}{Z} \right\rangle^n \quad (4)$$

and where the sign function  $\operatorname{sgn}$  is defined as

$$\operatorname{sgn}(x) = \begin{cases} 1, & x > 0, \\ 0, & x = 0, \\ -1, & x < 0, \end{cases} \quad (5)$$

The McCauley brackets  $\langle \cdot \rangle$  are here defined as

$$\langle x \rangle = \begin{cases} x, & x > 0, \\ 0, & x \leq 0. \end{cases} \quad (6)$$

The yield criterion is given by

$$f = |\sigma - \chi| - R - k \quad (7)$$

where  $R$  is the drag stress and  $k$  is the true elastic limit. The elastic domain is defined by  $f \leq 0$  and the inelastic domain by  $f > 0$ .

### 2.2 Hardening terms

#### 2.2.1 Kinematic hardening

The kinematic hardening  $\chi$  is used to capture directional dependent effects such as the Bauschinger effect due to the plastic flow under cyclic loading. In a three dimensional principal stress space, it corresponds to a translation of the elastic domain. It may have multiple terms as follows:

$$\chi = \sum_{i=1}^M \chi_i \quad (8)$$

The evolution equation of the back stress  $\chi_i$  is here defined as the sum of a linear hardening, dynamic recovery, and static recovery terms [4] [5]:

$$\dot{\chi}_i = C_i \dot{\epsilon}_p - \gamma_i \chi_i \dot{p} - \beta_i |\chi_i|^{r_i-1} \chi_i \quad (9)$$

While the linear hardening and dynamic recovery term govern the overall hysteresis loop shape, the static recovery term allows for stress relaxation to be simulated during strain holds [5].

#### 2.2.2 Isotropic hardening

The isotropic hardening  $R$  is used to describe directionally independent effects such as the change in the size of the yield surface during cyclic loading as for the cyclic hardening or for the cyclic softening. In a three dimensional principal stress space, it corresponds to an expansion or a contraction of the elastic domain around its origin. As for the kinematic hardening, it may have multiple terms as follows:

$$R = \sum_{j=1}^N R_j \quad (10)$$

The evolution of  $R_j$  follows the cumulated plastic strain  $p$ . Taking into account static recovery, the evolution equation of  $R_j$  for a non-linear isotropic hardening is here defined as [4]

$$\dot{R}_j = b_j (Q_j - R_j) \dot{p} - q_j R_j^{m_j} \quad (11)$$

For linear isotropic hardening, the evolution equation of  $R_j$  is

$$\dot{R}_j = R_{0,j} \dot{p} \quad (12)$$

with  $R_{0,j}$  is the asymptotic value of the isotropic hardening  $R_j$ .

### 2.3 Viscous behavior

A viscous overstress function is considered to describe the rate dependency of the stress. The rate dependency of the stress and therefore the creep effect is accounted for within the model in the form of the Norton creep law [6] as follows

$$\sigma_v = Z\dot{p}^{1/n} \quad (13)$$

where,  $\sigma_v$  is the viscous stress and  $Z$  and  $n$  are the viscous parameters.

At each moment the stress is given by

$$\sigma = \chi + \nu(R + k + \sigma_v) \quad (14)$$

where  $\nu = \text{sgn}(\sigma - \chi) = \pm 1$  according to the direction of the flow.

## 3 EXPERIMENTAL DATA

### 3.1 Performed tests

The identification of the Young's modulus, the true elastic limit and the parameters defining the kinematic hardening and isotropic hardening of the material are based on stress-strain measurements from uniaxial low cycle fatigue tests.

The determination of viscosity parameters and the static recovery parameters has been performed using time dependent stress measurements during uniaxial stress relaxation tests performed at high temperatures. A representative hold period has been considered for the stress relaxation tests.

In addition to the cyclic tests and the stress relaxation tests, uniaxial cyclic dwell tests with identical hold periods in tension and in compression have been carried out at high temperatures to provide experimental data for the assessment of the accuracy of the defined material parameters.

The uniaxial low cycle fatigue tests were performed up to failure in strain-controlled mode with a fixed total strain range of 2 %, strain ratio of -1, and at strain rate of 0.2 %/s. A trapezoidal wave form was used as the load path.

The uniaxial stress relaxation tests have been performed at strain levels increasing from 1 % to 6 % with increments of 1 %, a strain rate of 0.2 %/s, and hold periods of period of 600 s.

The uniaxial dwell tests have been performed in strain-controlled mode for a total strain range of 2 %, a strain ratio of -1, and a strain rate of 0.2 %/s. For every cycle, the strain has been holding at extreme values in tension and in compression for a period of 600 s.

The strain amplitude value of 1 % and the hold period of 600 s are quite representative of the load conditions of a combustion chamber wall in service.

### 3.2 Test specimen

Identical test samples have been used for the different tests. The shape and the dimensions of the rotatory-symmetric test specimens are illustrated in Figure 1.

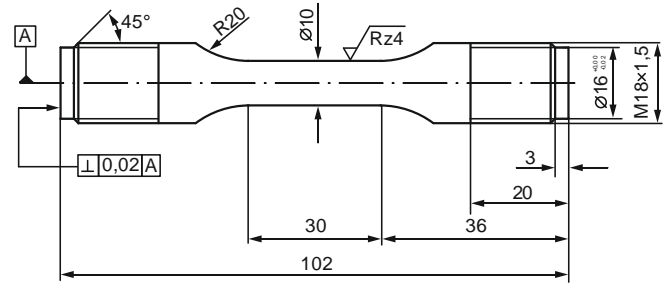


Figure 1. Drawing of the test specimen (geometry and dimensions in mm)

### 3.3 Presented data

Although various temperatures have been defined for the characterization of the mechanical behaviour of the investigated cost efficient copper alloy, only the results related to the temperature of 900 K, at which the viscous behaviour of the material should be significant, are reported in the present paper to illustrate the step-by-step procedure adopted to identify the unified Chaboche constitutive model's parameters of the tested copper alloy.

## 4 IDENTIFICATION OF THE PARAMETERS

### 4.1 Defined model

With the aim to keep the total number of parameters for the model reasonable, defining the kinematic hardening  $\chi$  as the sum of two non-linear kinematic hardening terms (see Eq. 9) was sufficient to catch the shape of the experimental hysteresis loops from the LCF tests. The kinematic hardening  $\chi$  is then defined as:

$$\chi = \sum_{i=1}^2 \chi_i = \chi_1 + \chi_2 \quad (15)$$

The first part of the kinematic hardening  $\chi_1$  describes the transient region of the inelastic deformation, while the second part  $\chi_2$  describes the behavior at greater inelastic deformations when  $\chi_1$  has reached its saturation value.

Due to the evolution of the stress range with the number of cycles from the LCF tests, the isotropic hardening  $R$  is defined as the sum of a non-linear isotropic hardening term  $R_1$  (Eq. 11) and a linear isotropic hardening term  $R_2$  (Eq. 12) as follows

$$R = \sum_{j=1}^2 R_j = R_1 + R_2 \quad (16)$$

While  $R_1$  describes the initial non-linear transient behavior of the isotropic hardening  $R$ ,  $R_2$  is the asymptotic value of the isotropic variable  $R$  at large values of cumulated plastic strain  $\rho$ .

## 4.2 Parameter estimation

The identification of the model's parameters is performed adopting a step-by-step procedure. Initial values of the parameters are estimated processing the experimental data. These initial values are then used in an optimization routine based on a nonlinear least square fit to get accurate and reliable optimized material parameters.

The estimation of the initial parameters requires representative, quality experimental data so that a given parameter may be estimated using the test results sensitive to that particular parameter.

For the estimation of the initial value of the Young's modulus  $E$ , the true elastic limit  $k$ , the kinematic hardening parameters  $C_1$ ,  $C_2$ ,  $\gamma_1$ , and  $\gamma_2$ , the isotropic hardening  $b$ ,  $Q$ , and  $R_0$  and the viscous parameters  $K$ , and  $n$ , the way to process the experimental data to get their values is shown in details in [7].

In order to simplify the model, the exponents of the recovery terms  $r_1$ ,  $r_2$ , and  $m_1$  are set to unity [8]. The static recovery is then controlled by the coefficients  $\beta_1$ ,  $\beta_2$ , and  $q_1$  whose initial values are set to 1e-3 for a copper-base alloy [8].

## 4.3 Parameter optimization

The initial parameters estimated are used as inputs in a step-by-step identification procedure to obtain an optimum set of parameters. The step-by-step identification procedure consists of "staggered" optimization of the groups of the parameters using the test results sensitive to that particular group of parameters. The flowchart in Figure 2 shows the details of the optimization procedure

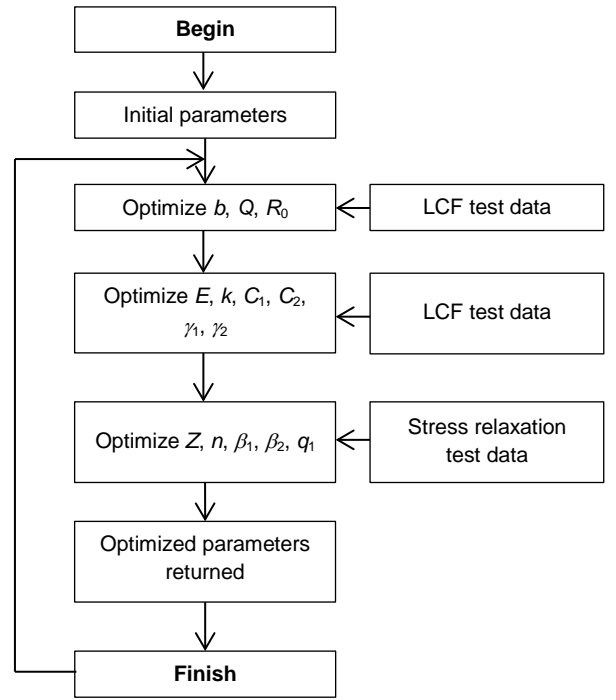


Figure 2. Flowchart of the step-by-step optimization procedure

## 4.4 Implementation in Matlab

### 4.4.1 Optimization procedure

The values of the model's parameters are optimized by fitting the experimental data based on the least-squares method. The principle of this optimization method is to search for the global minimum of the objective function defined as sum of the squares of the difference between the stress predicted by the model using the values of the parameters and the experimental measurements. The objective function is written as

$$F(x) = \frac{1}{2} \sum_{r=1}^Y (\sigma(x)_r^{num} - \sigma_r^{exp})^2 \quad (17)$$

$$x \in R^n \quad (18)$$

$$LB \leq x \leq UB \quad (19)$$

where  $x$  is the parameters set to be optimized (a vector of  $n$  components),  $\sigma(x)_r^{num}$  and  $\sigma_r^{exp}$  are the model predicted stress and the experimental measured stress, at a specific time  $r$ , within the test period.  $Y$  is the total number of experimental data points used in the optimization.  $LB$  and  $UB$  are the lower and upper boundaries of  $x$  allowed during the optimization.

#### 4.4.2 Optimization program development

An optimization program for processing the experimental data and determining the material parameters in the Chaboche unified viscoplastic model has been developed and implemented within Matlab, as in [2]. The flowchart in Figure 3 shows the main steps of the optimization process implemented within Matlab, where the ODE solving process is embedded within the non-linear least-squares algorithm-based optimization process (grey box).

The initial parameters estimated processing the experimental data are used as the input in the optimization program. The predicted stress value at every time step of the experimental data is calculating using the *ODE45* function corresponding to a certain set of model's parameters  $x_k$ .

The non-linear least-squares algorithm-based optimization process uses the *lsqnonlin* optimization function from Matlab to get the optimum set of parameters  $x^*$ .

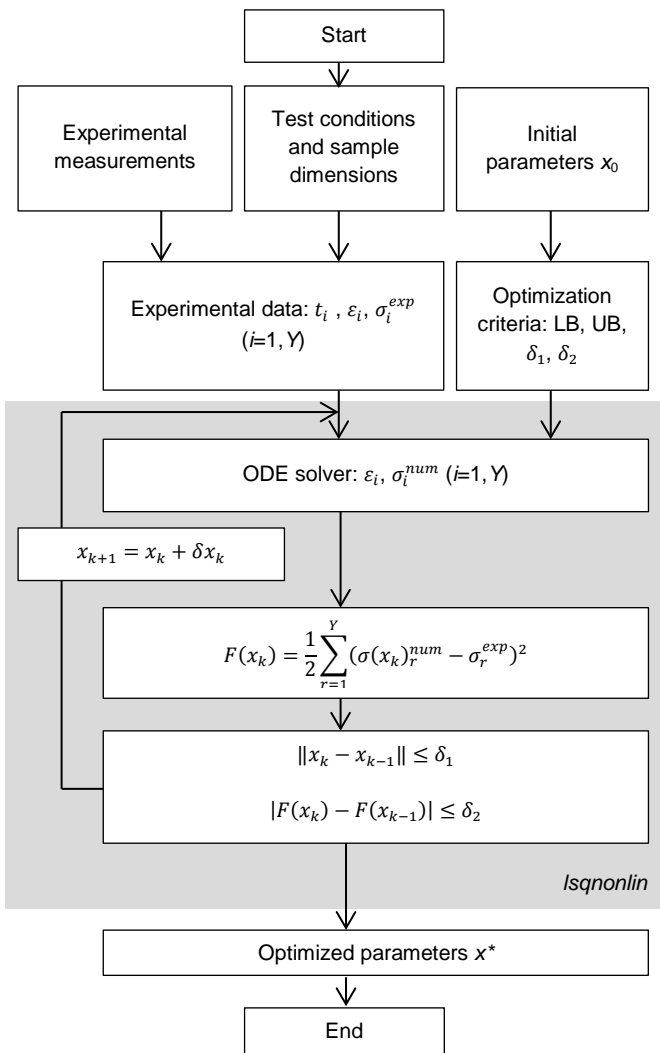


Figure 3. Flow chart of the optimization program developed and implemented within Matlab

relaxation test, tensile test, dwell test, etc.). As the material parameters are optimized in separate sets, the developed optimization program presented in Figure 3 below has been used in every optimization step of the optimization procedure presented in Figure 2.

## 5 COMPARISON OF THE MODEL PREDICTIONS TO THE EXPERIMENTAL DATA

The solution of the numerical model using the optimized material parameters is compared with the experimental data from uniaxial strain-controlled low cycle fatigue test, stress relaxation test with 600 s hold periods and strain-controlled dwell test with 600 s hold periods in tension and in compression at 900 K to assess the accuracy of the determined model's coefficients.

### 5.1 LCF test

The model simulation of the strain-controlled LCF test performed at a temperature of 900 K, a strain range of 2 % and a strain rate of 0.2 %/s is compared to the experimental measurement in Figure 4, Figure 5, and Figure 6 for the first, the 60<sup>th</sup> and 120<sup>th</sup> cycle, respectively. Globally, the shapes of the numerical hysteresis loops and experimental stress-strain curves show a relatively good coincidence. The good correlation between the simulation and the experimental data was obtained over the whole strain range and for all cycles.

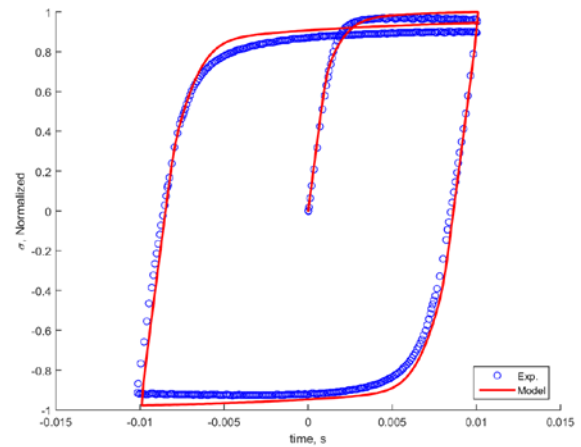


Figure 4. Simulation of the first cycle of the strain-controlled LCF test at 900 K

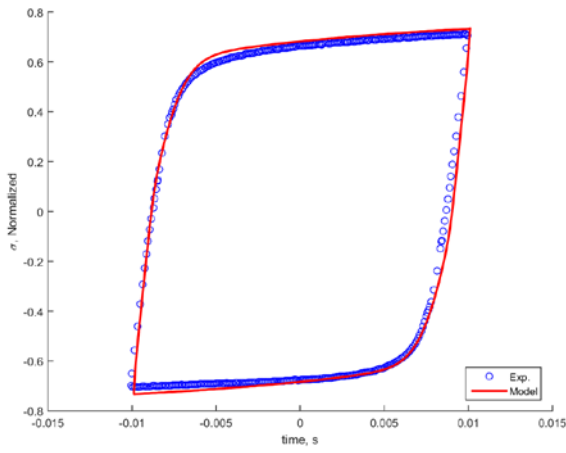


Figure 5. Simulation of the 60<sup>th</sup> cycle of the strain-controlled LCF test at 900 K

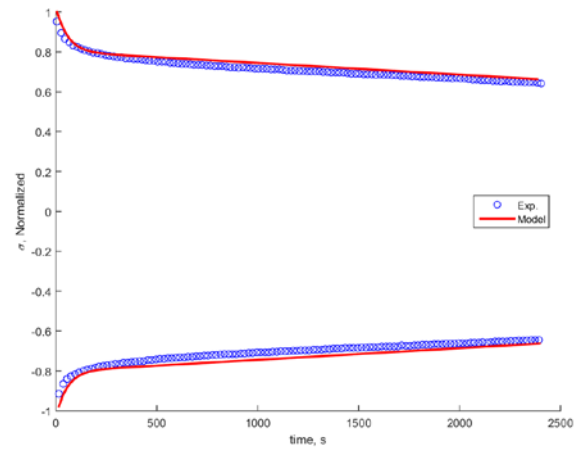


Figure 7. Simulation of the cyclic softening of the strain-controlled LCF test at 900 K

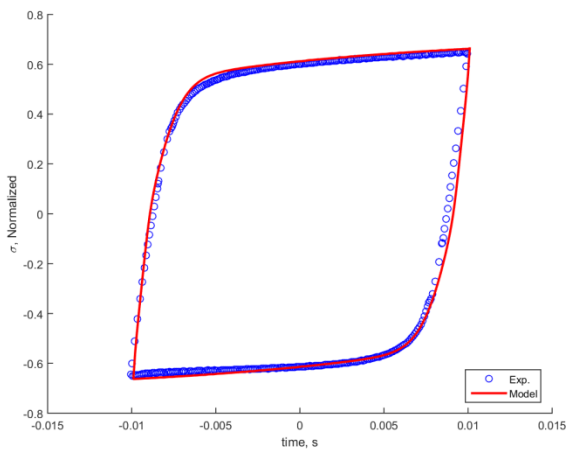


Figure 6. Simulation of the 120<sup>th</sup> cycle of the strain-controlled LCF test at 900 K

The ability of the model to predict cyclic softening of the material is investigated comparing the predicted evolution of the stress range throughout the cyclic life of the material to the measurements of the strain-controlled LCF test performed at 900 K. As shown in Figure 7, the different stages of the softening of the material are well depicted by the model. As observed experimentally, the model predicts an initial short and nonlinear transient reduction of the stress range for the first cycles followed by an almost steady decrease of the stress range with the running of the LCF test.

## 5.2 Stress relaxation test

Experimental data from the stress relaxation test performed at 900 K are used to assess the capability of the model to simulate the rate dependence and relaxation of the material.

The response of the model with and without considering static recovery is compared to the measurements in Figure 8. One can see that the model prediction of the stress relaxation is greatly enhanced by taking into account the static recovery since numerical value of the stress are in a better agreement with the experimental data. These results attest that time recovery may play a significant role at very low strain rates such as creep and cyclic loading with long hold periods, where viscous deformation prevails [9].

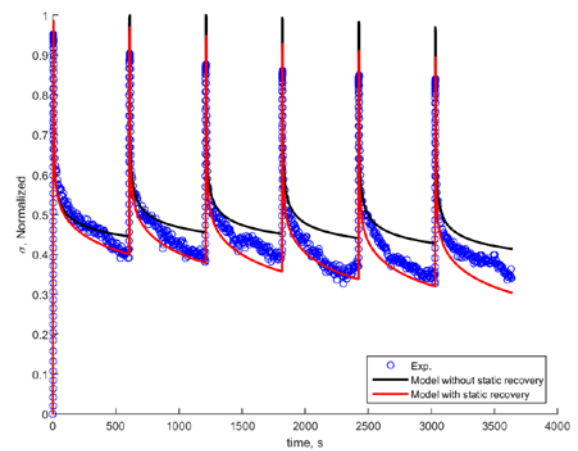


Figure 8. Simulation of the stress relaxation test with 600 s hold periods at 900 K with and without considering static recovery

### 5.3 Dwell test

In addition to the cyclic tests and the stress relaxation tests, a uniaxial cyclic dwell test with identical hold periods in tension and compression has been carried out at high temperatures to provide experimental data for the assessment of the accuracy of all defined parameter values.

In Figure 9, the stress evolution with time predicted by the numerical model is compared to the measurement of the stress during the dwell test performed at 900 K. The difference in the stress range value before the hold periods between the prediction of the model and the measurement is in part due to some scatter in the experiment data of the LCF test and the dwell test. The relaxation of the stress during the hold period in tension and compression is quite well simulated by the model although the model predicts a bit slower relaxation of the stress compared to the experiment. Globally, the correlation between the model prediction and the measured stress evolution is acceptable.

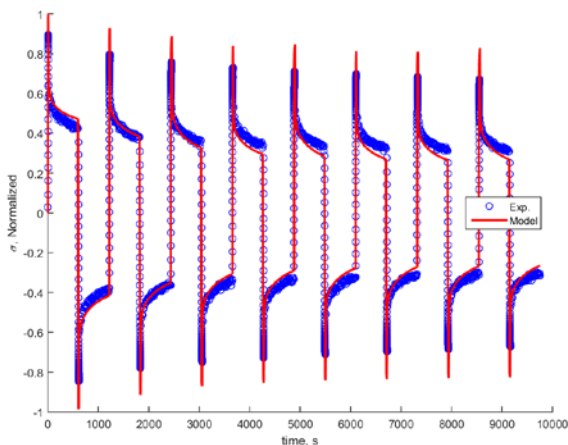


Figure 9. Simulation of the dwell test with 600 s hold periods in tension and in compression at 900 K.

## 6 CONCLUSION AND OUTLOOK

The unified Chaboche model with static recovery has been selected for the simulation of the mechanical behavior of a cost effective copper based alloy at high temperature.

Strain-controlled uniaxial low cycle fatigue tests and stress-relaxation tests have been used for the determination of the model's parameters. A step by step procedure has been defined to determine the values of the model's parameters.

The predictions of the model using the optimized parameters show a reasonably good agreement with the experimental data for the considered uniaxial tests.

Currently, work is being carried out to improve the accuracy of the prediction of the model by considering additional tests in the optimization procedure and upgrading the model to consider additional effects as thermal aging and damage.

## REFERENCES

- [1] J. Tong, Z. L. Zhan und B. Vermeulen, „Modelling of cyclic plasticity and viscoplasticity of a nickel-based alloy using Chaboche constitutive equations,” *International Journal of Fatigue* 26, pp. 829-837, 2004.
- [2] Y. P. Gong, C. J. Hyde, W. Sun und T. H. Hyde, „Determination of material properties in the Chaboche unified viscoplasticity model,” *Proc. IMechE Vol. 224 Part L: J. Materials: Design and Application*, pp. 19-29, 2009.
- [3] J. Chaboche und G. Rousselier, „On the plastic and viscoplastic constitutive equations (Part I and II),” *Journal of Pressure Vessel Technology* 105, pp. 153-159, 1983.
- [4] A. Ambroziak und P. Klosowski, „The elasto-viscoplastic Chaboche model,” *Task Quarterly*, Bd. 10, Nr. 1, pp. 49-61, 2006.
- [5] P. Pritchard, L. Carroll und T. Hassan, „Constitutive modeling of high temperature uniaxial creep-fatigue and creep-ratcheting responses of Alloy 617,” in *ASME 2013 Pressure Vessels and Piping Conference PVP 2013*, Paris, France, 2013.
- [6] F. H. Norton, *The creep of steel at high temperature*, New York: McGraw Hill, 1929.
- [7] W. Bouajila und J. Riccius, „Modelling of the mechanical behavior of a copper-base alloy using Chaboche model's constitutive equations,” in *6th European Conference for Aeronautics and Space Sciences (EUCASS)*, Krakow, Poland, 2015.
- [8] W. Schwarz, „Modelling of viscoplasticity, ageing, and damage for life prediction of rocket combustion chambers,” *Der Technischen Fakultät der Universität Erlangen-Nürnberg*, Erlangen, 2013.
- [9] J. Tong und B. Vermeulen, „The description of cyclic plasticity and viscoplasticity of waspalooy using unified constitutive equations,” *International Journal of Fatigue*, Bd. 25, pp. 413-420, 2003.